IJAREEIE

e-ISSN: 2278-8875
p-ISSN: 2320-3765

International Journal of Advanced Research

in Electrical, Electronics and Instrumentation Engineering

Volume 11, Issue 11, November 2022

ISSN INTERNATIONAL STANDARD SERIAL NUMBER INDIA

Impact Factor: 8.18

International Journal of Advanced Research in Electrical, Electronics and Instrumentation Engineering (IJAREEIE)

| e-ISSN: 2278 – 8875, p-ISSN: 2320 – 3765| www.ijareeie.com | Impact Factor: 8.18|

||Volume 11, Issue 11, November 2022||

|DOI:10.15662/IJAREEIE.2022.1111006 |

LVRT Capability of DFIG-Based Wind Turbines: Analysis and Control

Abdullah Eial Awwad

Assistant Professor, Department of Electrical Power Engineering and Mechatronics,

Faculty of Engineering, Tafila Technical University, Jordan

ABSTRACT: In this paper, the Low Voltage Ride Through (LVRT) capability of the doubly-fed induction generators (DFIG) based wind turbines is presented. Simulations were conducted to provide insight into the impact of different grid faults on DFIG wind turbines. MATLAB-Simulink software is used to simulate and assess the dynamic behavior of DFIG wind turbines during grid faults. Under voltage dip, DFIG is evaluated and analyzed with different conditions, such as symmetrical and asymmetrical grid faults. In this paper, the possible solutions for LVRT in order to meet grid-code requirements were presented. The crowbar protection circuit is used to protect 3.5 kW DFIG, and the results are compared. Therefore, connecting crowbar resistances in parallel with the machine rotor circuit will reduce the peaks generated due to voltage dips, and the reactive power is provided by the DFIG in this situation to meet grid codes.

KEYWORDS*:* Crowbar Protection, DFIG, LVRT, Wind Energy System, WindTurbine.

I. INTRODUCTION

In recent years, wind energy is considered the most promising form of renewable energy. The double-fed induction generator (DFIG) is widely used for variable-speed wind energy conversion systems (VS-WECS). The benefit of the DFIG over other variable-speed generators is that, unlike complete power converters used in synchronous generators, the power electronic components only need to handle only a third of the generating power [1,2]. To ensure high quality, and reliability, low-voltage ride-through (LVRT) and grid support capabilities are increasingly essential for grid-tied renewable energy sources. A need for LVRT indicates that wind power plants must stay connected even in the presence of transient grid voltage dips, thus maintaining the network voltage and frequency stability [3].

Several LVRT techniques have been discussed in the literature. The crowbar protection is the mostly used. In this context, the DFIG is operated as a conventional squirrel cage induction machine that absorbs reactive power from the faulted grid [4,5]. During the fault, to reduce the inrush currents in the rotor circuit and limit the DC-link overshoot voltage, advanced control approaches for the rotor and grid side converters are proposed in [6,7]. An efficient control technique to improve the fault ride-through (FRT) capability of DFIG during the symmetrical and asymmetrical grid faults is introduced in [8]. Furthermore, the stability of DFIG during FRT in the weak grid has been studied in [9]. The dynamic stability of DFIG-based VS-WEGS during asymmetric LVRT has been investigated in [10,11]. Another previous study proposed a new technique to determine the crowbar resistance of DFIG; the method was used to improve the FRT capability of the DFIG during the grid voltage dips. Furthermore, different methods, software, and hardware circuits have been carried out to improve the FRT capability of the DFIG during grid disturbance [12–14].

In this paper, the dynamic model of DFIG is presented. The LVRT capability of DFIG-based wind turbines is discussed and the crowbar protection circuit is applied to protect 3.5 kW DFIG. Connecting crowbar resistances in parallel with the machine rotor circuit reduce the peaks generated due to symmetrical and asymmetrical applied voltage dips, and the reactive power is still provided by the DFIG to meet grid codes.

II. MODELLING OF DFIG-BASED WECS

Doubly-fed induction generators (DFIG) are now frequently used in wind turbines. As shown in Figure 1, the system configuration of the DFIG-based WECS consists of a DFIG generator, a partial-scale back-to-back (BTB) power converter, a filter, and a power transformer. The stator of the DFIG is directly linked to the grid, while the rotor is supplied by a bidirectional converter that is likewise directly connected to the grid.

| e-ISSN: 2278 – 8875, p-ISSN: 2320 – 3765| www.ijareeie.com | Impact Factor: 8.18|

||Volume 11, Issue 11, November 2022||

|DOI:10.15662/IJAREEIE.2022.1111006 |

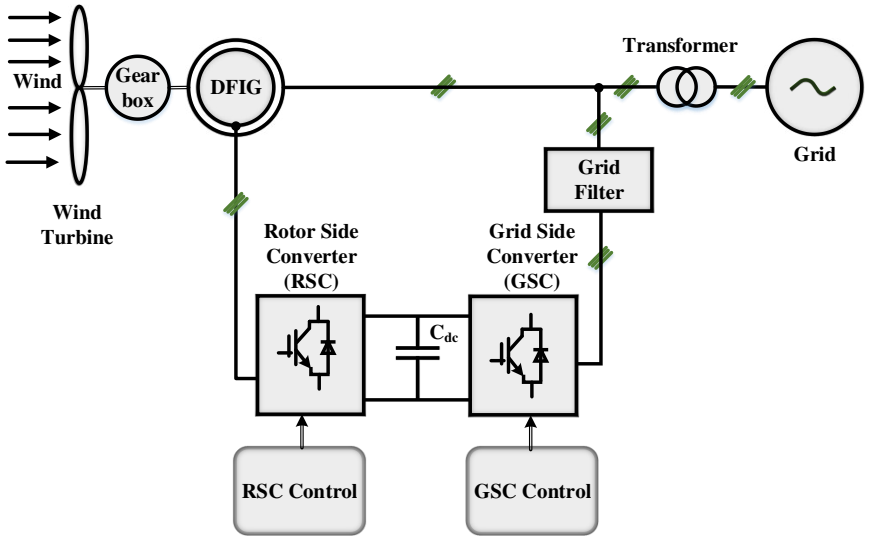

Figure 1: DFIG-based wind turbine configuration.

MATHEMATICAL DYNAMIC MODEL OF DFIG

Applying transformation under the synchronous rotating frame, the stator and rotor voltages equations of the d and q axes of the DFIG are as follows:

$$v_{ds} = R_s i_{ds} - \omega_s \varphi_{qs} + \frac{d}{ds}\varphi_{ds} \quad (1)$$

$$v_{qs} = R_s i_{qs} + \omega_s \varphi_{ds} + \frac{d}{ds}\varphi_{qs} \quad (2)$$

$$v_{dr} = R_r i_{dr} - \omega_r \varphi_{qr} + \frac{d}{ds}\varphi_{dr} \quad (3)$$

$$v_{qr} = R_r i_{qr} + \omega_r \varphi_{dr} + \frac{d}{ds}\varphi_{qr} \quad (4)$$

Where $v_s$and v_r are the stator and rotor voltages, i_s and i_r are the stator and rotor current, R_s and R_r are the resistance of the stator and rotor respectively, φ_s and φ_r are the stator and rotor angular frequencies. The subscripts d and q indicate that the variables are under d-axis and q-axis (synchronously rotating reference frame).
The stator and rotor flux equations can be described as follows:

$$\varphi_{ds} = L_s i_{ds} + L_m i_{dr} \quad (5)$$

$$\varphi_{qs} = L_s i_{qs} + L_m i_{qr} \quad (6)$$

$$\varphi_{dr} = L_m i_{ds} + L_r i_{dr} \quad (7)$$

$$\varphi_{qr} = L_m i_{qs} + L_r i_{qr} \quad (8)$$

where L_s, L_r, and L_m are the stator, rotor, and magnetizing inductances, respectively. The active (P_s) and reactive power (Q_s) of the stator and rotor can be expressed as follows:

$$P_s = \frac{3}{2}(v_{ds} i_{ds} + v_{qs} i_{qs}) \quad (9)$$

$$Q_s = \frac{3}{2}(v_{qs} i_{ds} - v_{ds} i_{qs}) \quad (10)$$

$$P_r = \frac{3}{2}(v_{dr} i_{dr} + v_{qr} i_{qr}) \quad (11)$$

$$Q_q = \frac{3}{2}(v_{qr} i_{dr} - v_{dr} i_{qr}) \quad (12)$$

Applying a single mass model, the mechanical model of the wind turbine can be written as follows:

$$T_m = J_{eq}\frac{d\omega_m}{dt} + B\omega_m + T_e \quad (13)$$

| e-ISSN: 2278 – 8875, p-ISSN: 2320 – 3765| www.ijareeie.com | Impact Factor: 8.18|

||Volume 11, Issue 11, November 2022||

|DOI:10.15662/IJAREEIE.2022.1111006 |

Where T_m is the turbine-driving torque (N·m);J_{eq} is the total equivalent moment of inertia of the turbine and generator (kg·m^2); B is the damping coefficient representing the turbine and generator rotational losses (N·m·s); andT_e is the electromagnetic torque of the generator (N·m). Based on the (1) to (12), the dynamic DFIG model is shown in Figure 2.

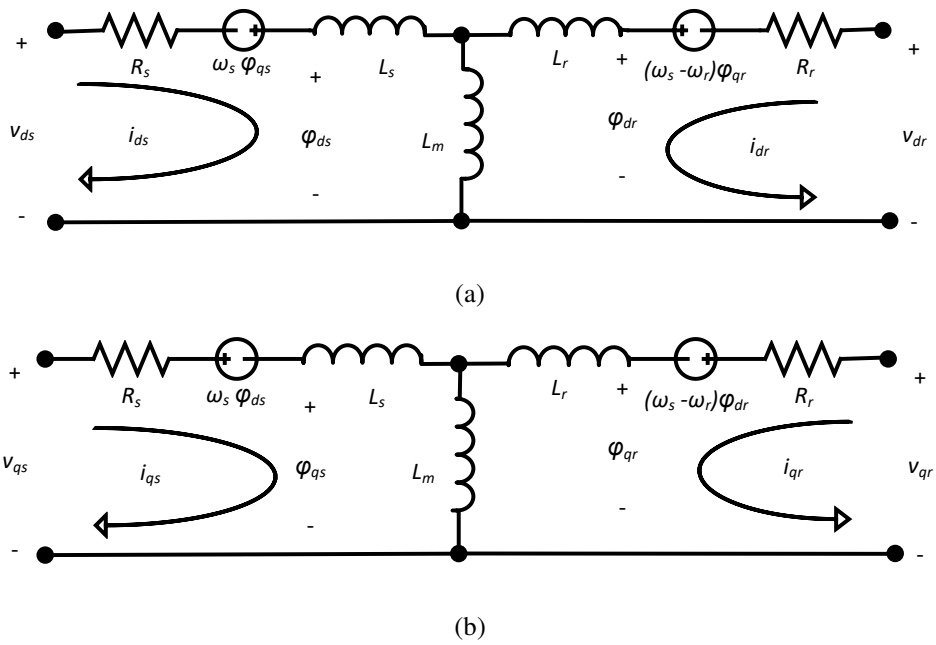

Figure 2: Equivalent dynamic model of DFIG

III. LVRT REQUIREMENT AND VOLTAGE DIP MODEL

In the DFIG-based wind turbine, the low-voltage ride-through (LVRT) capacity must be enhanced in order for it to remain connected to the grid during grid faults. Figure 3 depicts the LVRT requirements according to the National Electric Power Company (NEPCO) network code in Jordan [15]. Wind turbines remain connected and return to their rated value practically immediately after a significant voltage dips. As demonstrated, the generation system must remain linked to the grid for at least 250 ms even if the grid voltage drops to zero, and reactive current support is also necessary.

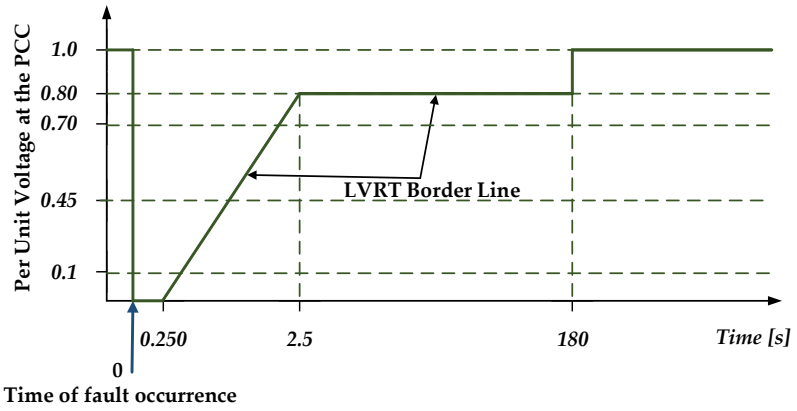

Figure 3: voltage at the PCC for LVRT characteristic provided by NEPCO [15].

In the three-phase system, different faults can occur, usually caused by short circuits. Simply, the grid fault with wind farms connected to the grid can be easily modeled as shown in Figure 4.

| e-ISSN: 2278 – 8875, p-ISSN: 2320 – 3765| www.ijareeie.com | Impact Factor: 8.18|

||Volume 11, Issue 11, November 2022||

|DOI:10.15662/IJAREEIE.2022.1111006 |

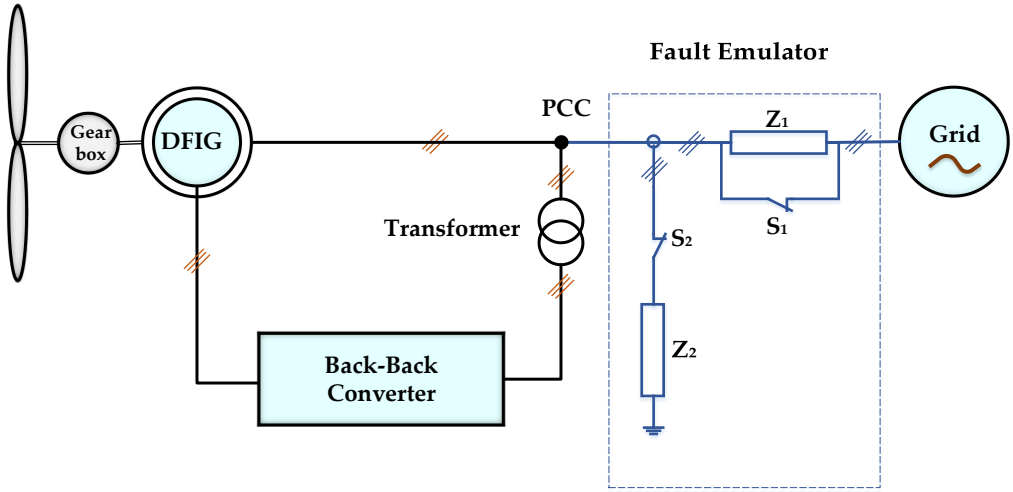

Figure 4: Fault emulator in DFIG-based WECS.

Assuming a grid fault occurs at point A, the grid voltage at the point of common coupling (v_{PCC}) can be written as:

$$v_{pcc} = \frac{z_f}{z_f + z_g} V_g \quad (14)$$

Where V_g is the grid voltage before the fault, Z_g is the grid impedance and the Z_f is the shunt impedance fault resistance.

IV. RESULTS AND DISCUSSION

1. DFIG WITHOUT CROWBAR PROTECTION:

In this work, a 3.5 kW DFIG was simulated using MATLAB/Simulink. The parameters of the 3.5 kW system are listed in Table 1.

Table 1: Parameters of 3.5 kW DFIG

Rated Power, P_{rated}	3.5 kW
Synchronous Speed, n_s	1500 rpm
Nominal Torque, T_n	23.7 N.m
Stator Voltage, V_s	380 V
Rotor Voltage, V_r	140 V
Stator Resistance, R_s	996.9 mΩ
Rotor Resistance, R_r	268.8 mΩ
Mutual Inductance, L_m	2.5 mH
Stator inductance, L_s	0.199 mH
Rotor Inductance, L_r	254.341 mH

In the simulation, different types of faults, symmetrical and asymmetrical faults, were investigated and compared:

| e-ISSN: 2278 – 8875, p-ISSN: 2320 – 3765| www.ijareeie.com | Impact Factor: 8.18|

||Volume 11, Issue 11, November 2022||

|DOI:10.15662/IJAREEIE.2022.1111006 |

A- SINGLE-PHASE FAULT:

In this case, to evaluate the dynamic performance of the DFIG, a 10% and 80% voltage dip were applied to the fault point. The first fault started at t= 0.8 ms and the second fault started at 1.6 ms. Both of them have remained for 250 ms. Figure 5 shows the dynamic performance of the DFIG, including the grid voltage (V_{grid}), current of the rotor (I_{rotor}) and stator current (I_{stator}), the flux of the rotor (φ_{rotor}), the flux of stator (φ_{stator}), and the electromagnetic torque (T_{em}). As shown, an overcurrent was observed in the rotor key waveform. Compared with the nominal values, the rotor current shows an increase of around 200 %, and increasing around 150 % was observed in the stator current. As expected, as the voltage dip decreased, the overcurrent amplitude also decreased.
Moreover, the torque has a notable change in performance, see Figure 5. This is mainly due to the flux of the dq-components, e.g. φ_{qr}andφ_{qs} are affected during this type of fault, see Figure 5.

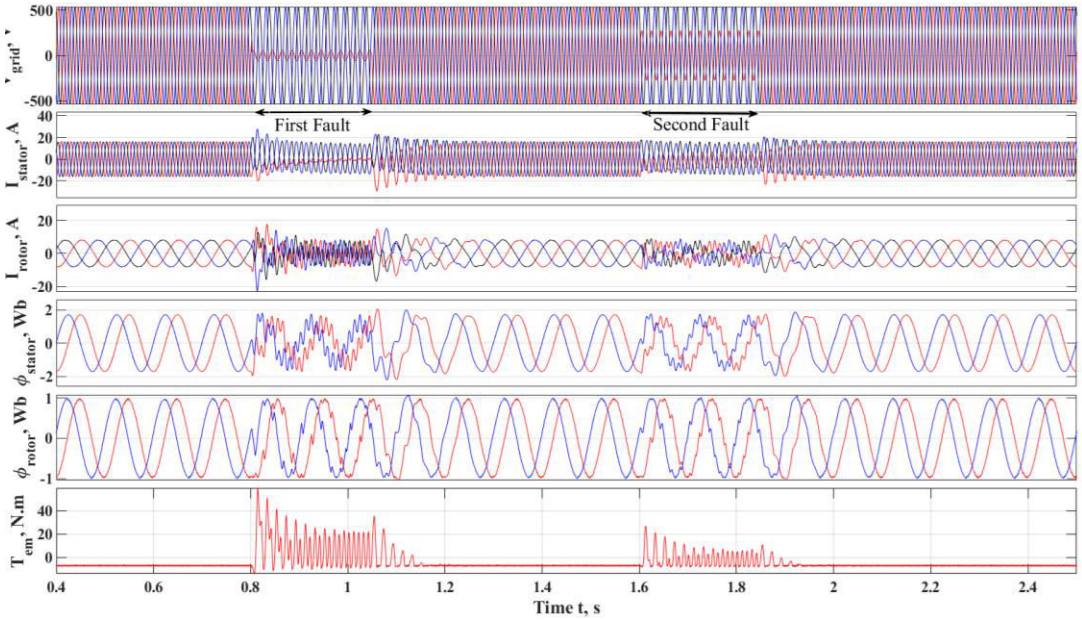

Figure 5: main waveforms of a single-phase fault in DFIG-based WECS configuration.

B- Three-Phase Fault:

In this type of fault, all three phases are shorted together. A 10% and 80% voltage dip were applied to the fault point. The first fault started at t= 0.8 ms and the second fault started at 1.6 ms. The simulation waveforms are depicted in Figure 6. Like the case of a single-phase fault, an overshoot in the rotor current was observed. More, the rotor and stator fluxes are affected by the fault, and hence the torque shows unstable performance as shown in Figure 6.

| e-ISSN: 2278 – 8875, p-ISSN: 2320 – 3765| www.ijareeie.com | Impact Factor: 8.18|

||Volume 11, Issue 11, November 2022||

|DOI:10.15662/IJAREEIE.2022.1111006 |

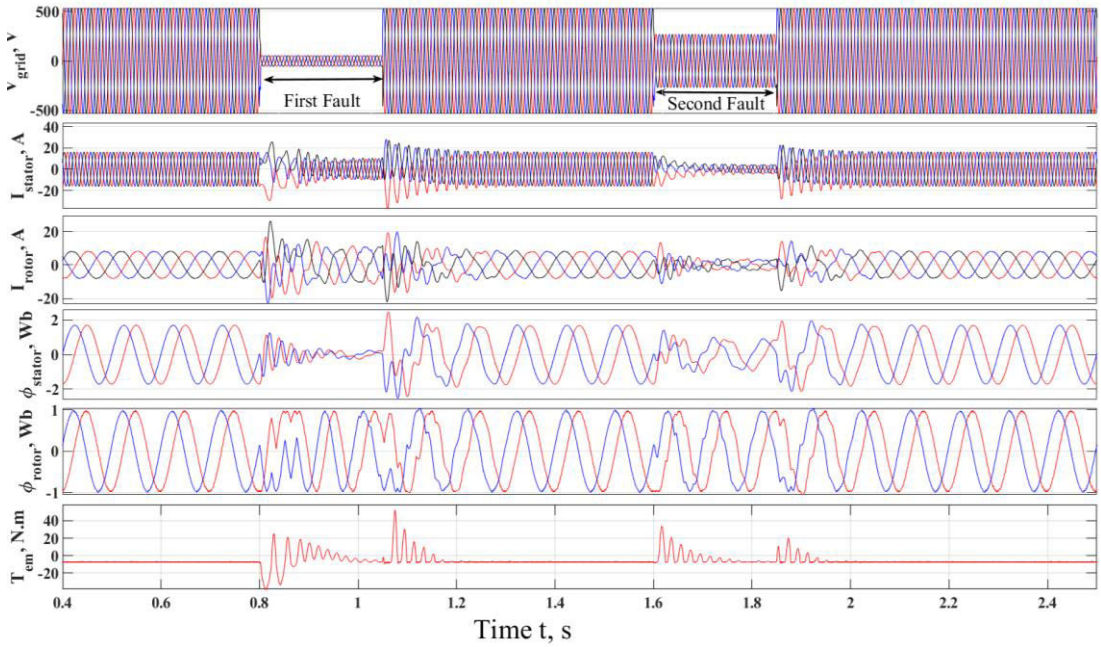

Figure 6: main waveforms of a three-phase fault in DFIG-based WECS configuration.

2. DFIG WITH CROWBAR PROTECTION (With Rotor-Side Crowbar):

In this paper, the rotor-side crowbar method is used for the LVRT of DFIG. The control methodology of the rotor-side crowbar is presented in Figure 7. The design and control of crowbars is a key topic of current research. In this context, the crowbar is applied to protect the RSC from the transient voltage and current. As dip voltage occurs, the rotor overcurrent is detected, and/or the DC-link voltage is exceeded the rated limitation. Thus the crowbar is enabled and the rotor is shorted hence the rotor circuit is disabled, i.e. DFIG operates as a cages generator. As shown in Figure 7, the crowbar is typically made up of three-phase switches and a three-phase resistor.

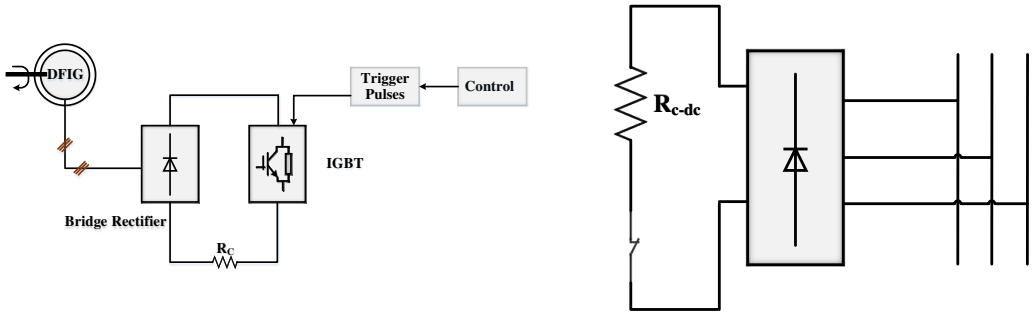

(a) (b)

Figure 7: Rotor-side crowbar (a) active protection and (b) DC-side resistor

As discussed in [16], the relationship of the crowbar resistance in the three-phase crowbar R_c and DC-switch crowbar $R_{c\text{-}dc}$ can be expressed as follows:

$$R_c = \frac{\sqrt{3}}{2} R_{c-dc} \qquad 15$$

In this work, Firstly different crowbar resistances were applied and then an optimal value is selected based on the overshoot values of the voltage and current. Figure 8 shows the simulation results of the DFIG at speed of 1200 rpm

| e-ISSN: 2278 – 8875, p-ISSN: 2320 – 3765| www.ijareeie.com | Impact Factor: 8.18|

||Volume 11, Issue 11, November 2022||

|DOI:10.15662/IJAREEIE.2022.1111006 |

under different single-phase voltage dips. As the crowbar protection is applied to the rotor circuit of the DFIG, the overshoot values will be reduced compared to those without the crowbar protection. Further, the DFIG is simulated under single-phase fault with different crowbar resistances and under different three-phase voltage dips, see Figure 9.

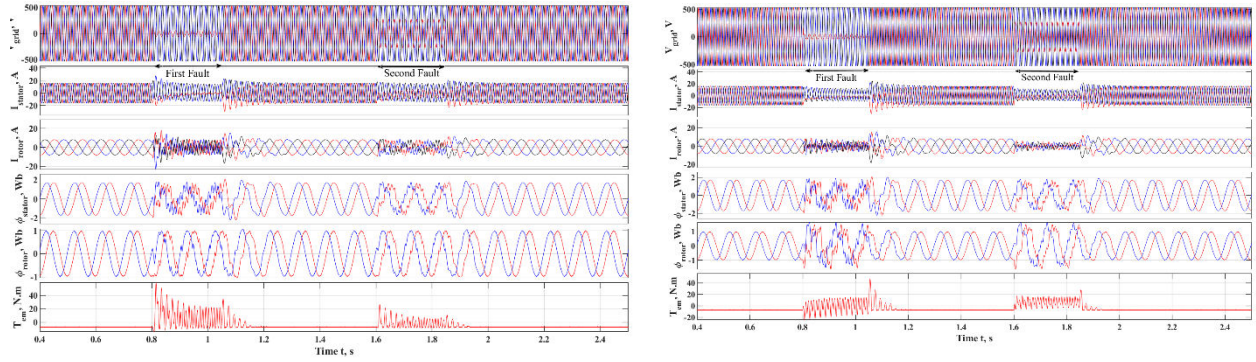

(a) (b)

Figure 8: main waveforms of a single-phase fault in DFIG-based WECS configuration: (a) without crowbar and (b) with crowbar protection.

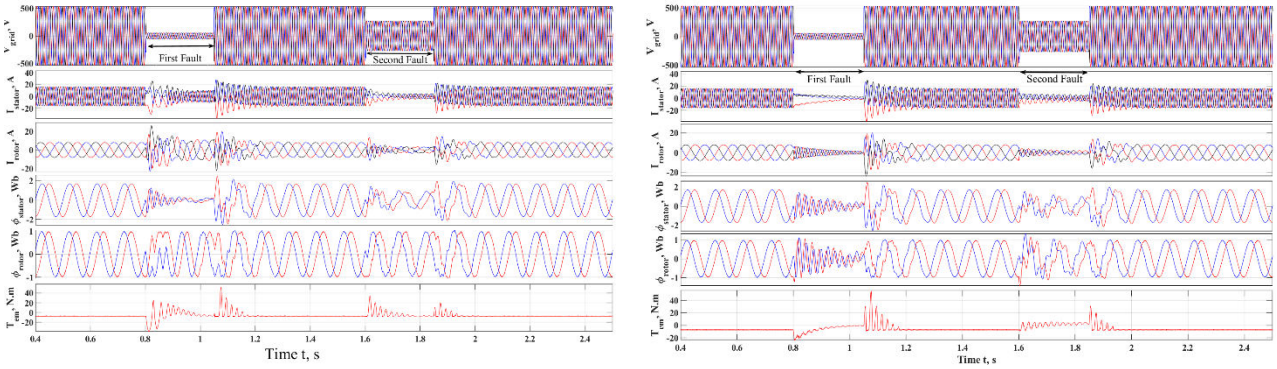

(a) (b)

Figure 9: main waveforms of a three-phase fault in DFIG-based WECS configuration: (a) without crowbar and (b) with crowbar protection.

Furthermore, as shown in Figure 10, different crowbar resistances are applied and hence the peak values in the different waveforms are minimized compared to those with other crowbar resistance values.

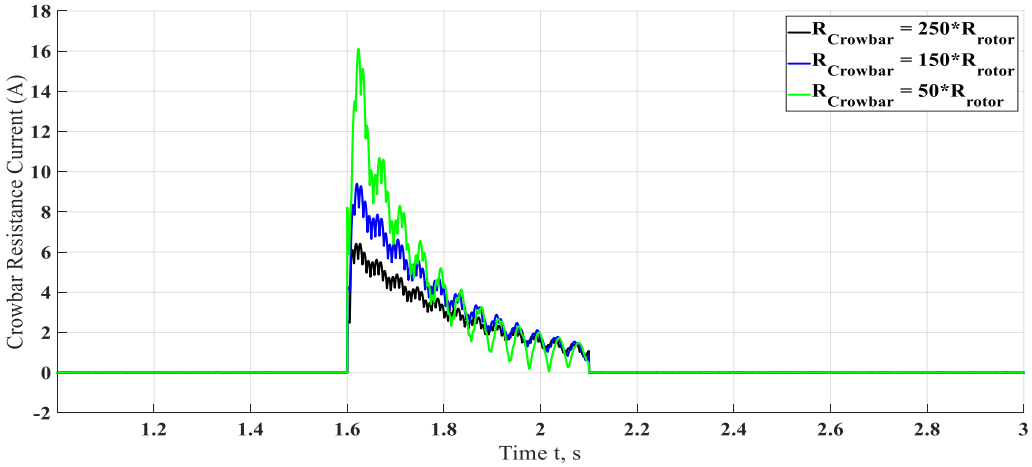

Figure 10: Crowbar current during three phase voltage dip using different crowbar resistances

| e-ISSN: 2278 – 8875, p-ISSN: 2320 – 3765| www.ijareeie.com | Impact Factor: 8.18|

||Volume 11, Issue 11, November 2022||

|DOI:10.15662/IJAREEIE.2022.1111006 |

IV. CONCLUSION

The behavior of DFIG under voltage dip was investigated in this paper for various fault types. The findings showed that the voltage dip has an impact on DFIG performance and that when a fault occurs, there are overvoltage and overcurrent on the rotor circuit in addition to electromagnetic torque instability. In this work, the LVRT risk solution was also covered, and the crowbar circuit was decided upon. The crowbar protection performed well in minimizing voltage, current, flux, and torque overshoots. The outcomes of applying various crowbar resistance levels were compared in order to select the best value. In future work, interesting points associated with the LVRT problem can be investigated and experimentally evaluated, e.g. series dynamic braking resistor and DC braking chopper.

REFERENCES

1. Xu, D.; Blaabjerg, F.; Chen, W.; Zhu, N.*Modelling and control of doubly fed induction generator wind power system under non-ideal grid*, 1st; Wiley-IEEE Press: Hoboken, 2016, ISBN 9781119172079.
2. EialAwwad, A. Dynamic Performance Enhancement of a Direct-Driven PMSG-Based Wind Turbine Using a 12-Sectors DTC.*WEVJ***2022**, *13*, 123, doi:10.3390/wevj13070123.
3. Ibrahim, R.A.; Zakzouk, N.E. A PMSG Wind Energy System Featuring Low-Voltage Ride-through via Mode-Shift Control.*Applied Sciences***2022**, *12*, 964, doi:10.3390/app12030964.
4. Yang, L.; Xu, Z.; Ostergaard, J.; Dong, Z.Y.; Wong, K.P. Advanced Control Strategy of DFIG Wind Turbines for Power System Fault Ride Through.*IEEE Trans. Power Syst.***2012**, *27*, 713–722, doi:10.1109/TPWRS.2011.2174387.
5. Din, Z.; Zhang, J.; Zhu, Y.; Xu, Z.; El-Naggar, A. Impact of Grid Impedance on LVRT Performance of DFIG System With Rotor Crowbar Technology.*IEEE Access***2019**, *7*, 127999–128008, doi:10.1109/ACCESS.2019.2938207.
6. Hansen, A.D.; Michalke, G. Fault ride-through capability of DFIG wind turbines.*Renewable Energy***2007**, *32*, 1594–1610, doi:10.1016/j.renene.2006.10.008.
7. Rahimi, M.; Parniani, M. Transient Performance Improvement of Wind Turbines With Doubly Fed Induction Generators Using Nonlinear Control Strategy.*IEEE Trans. Energy Convers.***2010**, *25*, 514–525, doi:10.1109/TEC.2009.2032169.
8. Mohammadi, J.; Afsharnia, S.; Vaez-Zadeh, S. Efficient fault-ride-through control strategy of DFIG-based wind turbines during the grid faults.*Energy Conversion and Management***2014**, *78*, 88–95, doi:10.1016/j.enconman.2013.10.029.
9. Hu, J.; Wang, B.; Wang, W.; Tang, H.; Chi, Y.; Hu, Q. Small Signal Dynamics of DFIG-Based Wind Turbines During Riding Through Symmetrical Faults in Weak AC Grid.*IEEE Trans. Energy Convers.***2017**, *32*, 720–730, doi:10.1109/TEC.2017.2655540.
10. Fang, X.; Yao, J.; Liu, R.; Zhao, Y.; Sun, P.; Huang, S. Small-Signal Stability Analysis and Current Control Reference Optimization Algorithm of DFIG-Based WT During Asymmetric Grid Faults.*IEEE Trans. Power Electron.***2021**, *36*, 7750–7768, doi:10.1109/TPEL.2020.3042514.
11. Guan, L.; Yao, J. Small-Signal Stability Analysis of Weak-Grid-Connected DFIG-based WT during Asymmetric Faults. In*2021 International Conference on Power System Technology (POWERCON)*. 2021 International Conference on Power System Technology (POWERCON), Haikou, China, 08/12/2021 - 09/12/2021; IEEE, 2021; pp 1601–1605, ISBN 978-1-6654-0737-3.
12. Chen, W.; Xu, D.; Chen, M.; Blaabjerg, F. Comparison of control strategies for DFIG under symmetrical grid voltage dips. In*IECON 2013 - 39th Annual Conference of the IEEE Industrial Electronics Society*. IECON 2013 - 39th Annual Conference of the IEEE Industrial Electronics Society, Vienna, Austria, 10/11/2013 - 13/11/2013; IEEE, 2013; pp 1542–1547, ISBN 978-1-4799-0224-8.
13. Al-Quteimat, A.; Niewienda, C.; Schafer, U. Low voltage ride through of doubly fed induction generator in wind power generation using crowbar solution. 2017 International Conference on Optimization 2017. In ; pp 667–674.
14. Ibrahim, N.Z.; Al-Quteimat, A.; Mozumdar, M.; Al Jufout, S. A novel approach for crowbar resistance determination for doubly fed induction generators in wind energy conversion systems.*International Journal of Ambient Energy***2022**, *43*, 4102–4111, doi:10.1080/01430750.2021.1874519.
15. NEPCO.*Intermittent Renewable Resources (IRR) Wind & PV Transmission Interconnection Code (TIC)*, 2015.
16. *Advanced control of doubly fed induction generator for wind power systems;*John Wiley & Sons Inc: Hoboken, New Jersey, copyright 2018, ISBN 9781119172062.

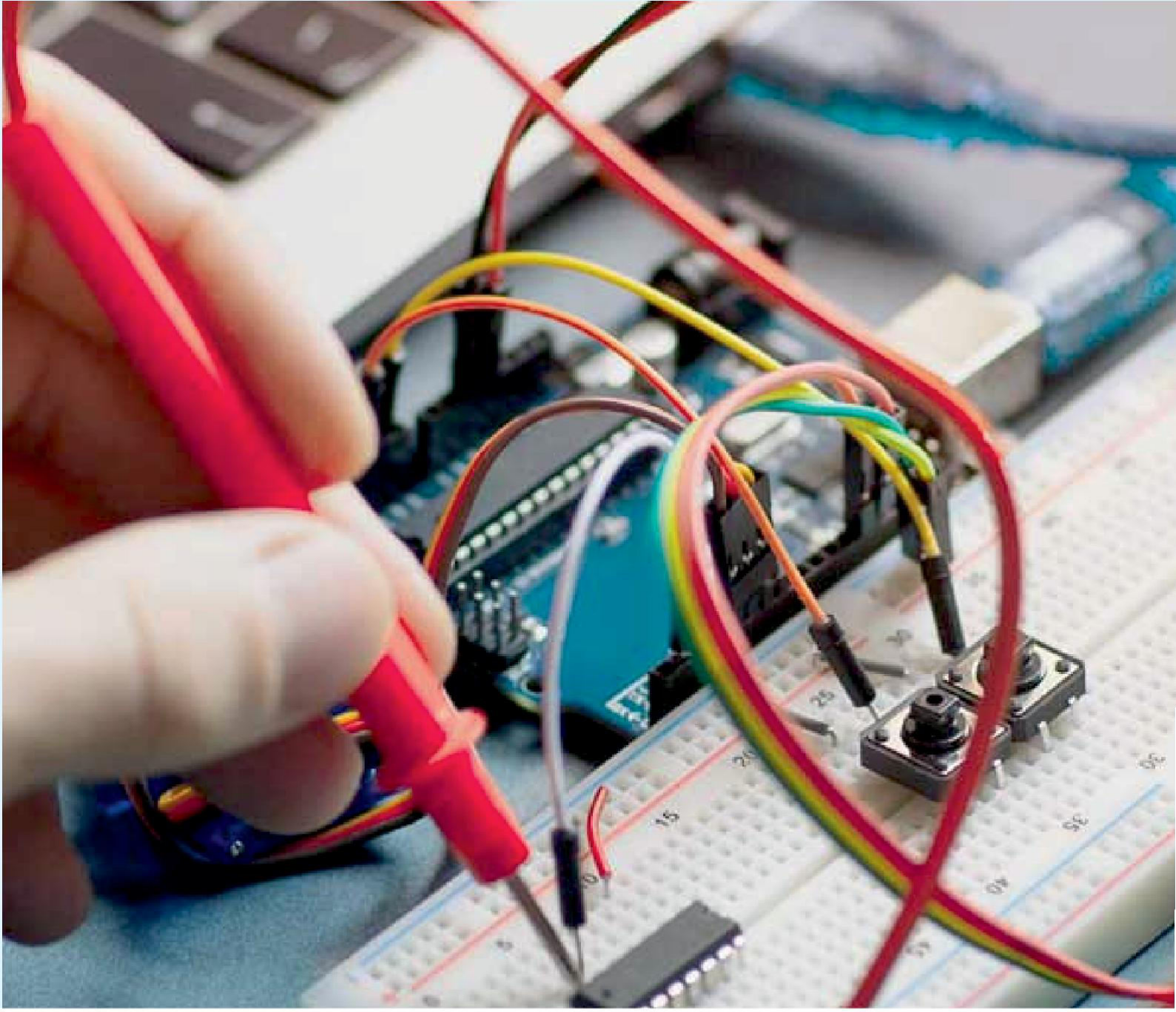

INNO SPACE
SJIF Scientific Journal Impact Factor

doi cross ref

ISSN INTERNATIONAL STANDARD SERIAL NUMBER INDIA

निस्केयर NISCAIR

Impact Factor: 8.18

International Journal of Advanced Research

in Electrical, Electronics and Instrumentation Engineering

9940 572 462 6381 907 438 ijareeie@gmail.com

www.ijareeie.com

Scan to save the contact details